Tracing and Dissecting How LLMs Recall Factual Knowledge For Real World Questions

Anonymous ACL submission

Abstract

Recent advancements in large language models (LLMs) have shown promising ability to perform commonsense reasoning, bringing machine closer to human-like understanding. However, deciphering the internal reasoning processes of LLMs remains challenging due to the complex interdependencies among generated tokens, especially in practical question-answering. In this study, we introduce a two-dimensional analysis framework—comprising token back-tracing and individual token decoding—to uncover how LLMs conduct commonsense reasoning. Through explanatory analysis of three typical reasoning datasets, we identify a consistent three-phase pattern: Subject Augmentation and Broadcasting, Object Retrieval and Reranking, and Conclusion Fusion and Generation. Our findings reveal that LLMs do not lack relevant knowledge but struggle to select the most accurate information based on context during the retrieval and rerank phase. Leveraging these findings, we apply representation engineering and selective fine-tuning to target specific modules responsible for retrieval and rerank errors. Experimental results show large improvements in response accuracy for both in-domain and out-of-domain settings, validating the rationality of the interpreting result.

1 Introduction

Recent progress in large language models (LLMs) have pushed machines closer to achieving human-like capabilities (Krause and Stolzenburg, 2023; Zhou et al., 2020). These models can not only comprehend user queries, but also perform commonsense reasoning based on factual knowledge. As a result, uncovering these abilities has become a focal point of interest. It is crucial for interpreting model behavior and analyzing unexpected errors (e.g., reversal curse (Berglund et al., 2023)), ultimately overcoming the limitations of LLMs.

Research on interpreting LLMs (Geva et al., 2023; Wang et al., 2024; Dai et al., 2022; Xie et al., 2024) often simplifies reasoning by focusing on factual triplets like "*Ganesha is a Hindu god*". These studies examine how models derive the object ("*Hindu*") from the subject ("*Ganesha*") as well as the relation ("*is*"). However, in real-world scenarios, model must go beyond these triplets to understand the question, select relevant facts, and synthesize information to provide an answer. For example, when asked, "*Is Ganesha associated with Thor?*", the model must grasp the context, recognize that "*Ganesha is a Hindu god*" from all Ganesha-related facts, and conclude they are not related. In contrast, for the question, "*Does Ganesha look like a tiger?*", the model in turn focuses on appearance-related facts, such as "*Ganesha is depicted with an elephant head*". Understanding how models select appropriate factual knowledge and analyze it to reach conclusions is crucial for comprehending their overall reasoning process. This holistic approach should extend beyond simple triplet analysis and can better reflect the complexity of real-world reasoning tasks.

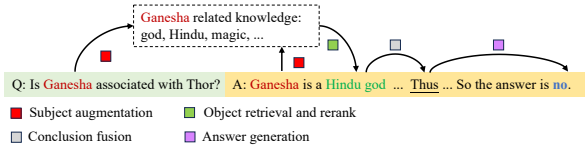

Figure 1: Model inner reasoning process on commonsense reasoning tasks.

In this study, we aim to decipher the commonsense reasoning process within the response of LLMs. The challenge lies in the dense interconnectivity of token generation, where each generated token is influenced by multiple preceding ones, leading to a recursive analytical complexity. To address this, we break down the analysis into two dimensions: token back-tracing and individual token decoding. Token back-tracing starts from the model's answer and traces back to the original question. It

identifies intermediate key tokens with significant direct impact through causal analysis. This reveals a chain of crucial information transfers between tokens, as shown in Fig. 1. For individual token decoding, we adopt an "explain then verify" strategy following Wang et al. (2023). Specifically, logit attribution (nostalgebraist, 2021) is applied to examine information changes within modules across layers. Then Sparse Autoencoder (SAE) (Gao et al., 2024) and knockout (Wang et al., 2023) techniques are used to verify by comparing the model's behavior with and without specific information.

Our interpreting analysis of three typical reasoning datasets revealed a consistent pattern in models' commonsense reasoning. The process unfolds in three phases: 1) **Subject augmentation and broadcast**: Firstly, the model generates extensive subject-related information through attention heads and MLP, and broadcasts it to subsequent key positions (e.g., sentence endings); 2) **Object retrieval and rerank**: the model retrieves the previously generated subject information with attention heads and reorders it using MLPs when predicting attributes.; and 3) **Conclusion fusion and generation**: the attributes are further transported to the conclusion through heads and generate corresponding conclusions, ultimately forming the answer. Based on this pattern, we further analyzed the failure cases of current models. One key finding is that *LLMs are not unaware of relevant facts, but rather struggle to select the most accurate fact during retrieval and rerank based on contextual cues*. This motivated us to develop a direct application of interpretability findings: by identifying specific modules through explanatory localization, we employed selective fine-tuning and representation engineering to optimize the attribute retrieval and rerank. Results show significant improvement in model performance, simultaneously validating the rationality of the interpretability results.

We summarize our contributions as follows: (1) We focus on interpreting the process of commonsense reasoning within LLMs into steps that are comprehensible to humans. Through experimental analysis, we found that LLMs first augment related facts and broadcast the information into the proceeding key positions, subsequently retrieving and re-ranking these facts to predict correct object, and finally fusing and generating conclusions and answers. (2) Building on the above observations, we further identify that on commonsense reasoning tasks, LLMs often fail to retrieve and rerank correct facts, leading to erroneous reasoning or conclusions. By selectively fine-tuning key heads and MLPs, the performance of reasoning is enhanced, especially for out-of-domain samples. It validates the reliability of the interpreting results.

2 Related Works

2.1 Mechanistic Interpretability

Mechanistic interpretability aims to understand model behavior by reverse-engineering the internal computational processes. One widely used technique is logit attribution (nostalgebraist, 2021), which projects internal vectors into the vocabulary space to interpret the information encoded within these representations. Several studies (Geva et al., 2021b, 2022; Dar et al., 2023; Belrose et al., 2023) have utilized this method to uncover a variety of interpretability results. Another prominent tool is activation patching (Meng et al., 2022; Wang et al., 2023; Goldowsky-Dill et al., 2023; Conmy et al., 2023), which applies causal interventions to internal model components using corrupted inputs. By examining the resulting changes in model predictions, this approach identifies critical modules and uncovers computational circuits. Numerous works (Lieberum et al., 2023; Zhang et al., 2024; Chen et al., 2024; Hanna et al., 2023) have successfull identified task-specific modules in LLMs using this method. In addition, sparse autoencoders (Bricken et al., 2023; Templeton et al., 2024; Lieberum et al., 2024; Gao et al., 2024) have been employed to decompose internal features into interpretable feature combinations. In this work, we integrate these tools to identify and analyze the modules responsible for commonsense reasoning.

2.2 Model reasoning ability Interpretation

Numerous studies have employed interpretability tools to investigate model mechanisms in reasoning tasks. Geva et al. (2023) explored factual knowledge recall, finding that subject information is enriched in the subject token in early layers, while relation information is passed to the final token, which then uses attention heads to extract the corresponding attribute from the subject representation. Building on this, Wang et al. (2024); Dai et al. (2022); Yu and Ananiadou (2024); Geva et al. (2022) identified MLP neurons involved in factual knowledge recall and demonstrated how modulating their activations can control model behavior. Additionally, works such as Yu et al. (2024); Ortu

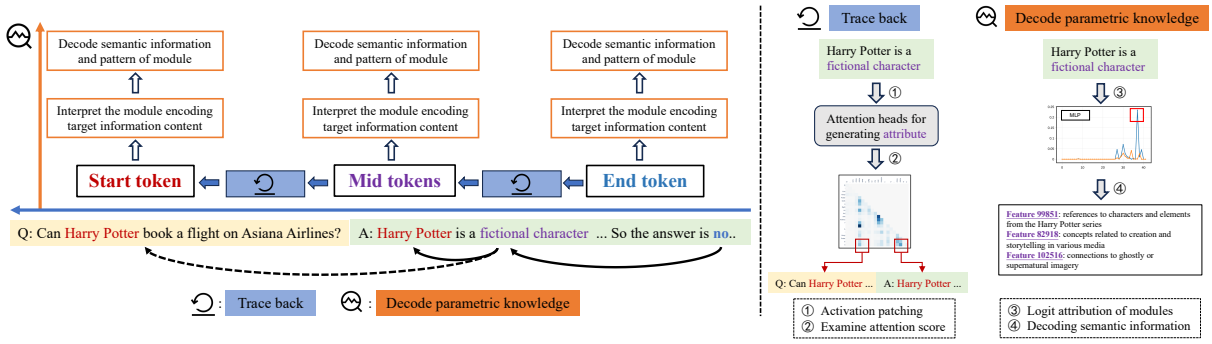

Figure 2: Overview of interpreting pipeline: 1) **Tracing back (horizontal)**: we use activation patching to identify the head with causal effect and trace the origin of the information iteratively. 2) **Decoding concept knowledge (vertical)**: we use logit attribution to identify the key module for generating concepts during reasoning at the key position and decode the semantic information within in it.

et al. (2024); Yu et al. (2023); Xie et al. (2024) analyzed the balance between retrieved knowledge and parametric memory. Dutta et al. (2024); Hou et al. (2023) examined model mechanisms in reasoning generation tasks. These studies largely focus on elementary retrieval tasks, such as recalling a single fact o from a triplet (s, r, o). In this study, we focus on interpreting the model reasoning process in more complicated commonsense reasoning tasks.

3 Methods

3.1 Preliminary

In our experiments, we uncovered several key token positions in the reasoning process through back tracing: *Subject*, *Object*, *Answer*. These tokens are observed special in experiments and therefore highlighted for better comprehension. (1) **Subject** ($\mathcal{S}$): The subject of inquiry in the question; this is a concept node in a knowledge graph (Speer et al., 2017), representing any entity, idea, or object relevant to commonsense (e.g., "*Harry Potter*" in Figure 2). (2) **Object** ($\mathcal{O}$): The object, paired with $\mathcal{S}$ contains some factual knowledge, is also a concept node. These objects, according to their relevance as accurate fact for the question, can be categorized into predicted objects $\mathcal{O}_p$ (e.g., "*Harry Potter is a 'fictional character'*") and candidate objects $\mathcal{O}_c$ (e.g., "*Harry Potter is a 'wizard'*"). (3) **Answer** ($\mathcal{A}$): The answer to the question, which varies based on the type of question. It may be a binary judgment (e.g., "*yes/no*") or a selection (e.g., "*(2) Kayla*"). We denote the correct and false answers as $\mathcal{A}_t$ and $\mathcal{A}_f$.

Furthermore, through back-tracing, we identified several positions that entail reasoning-related information: (4) **Reasoning conjunctive adverb** ($\mathcal{R}$): we find conjunctive adverbs that connect reasoning steps (e.g., "*Thus*") encodes rich information related to the answer. (5) **Conclusion** ($\mathcal{C}$): terms that convey the affirmative or negating essence of the conclusion sentence, clarifying the stance to the question. (e.g., "*cannot*" in "*Thus, Harry Potter cannot book a flight on Asiana Airlines.*") (6) **Question end** ($\mathcal{Q}_e$): we find abundant subject-related information is encoded at the end of question.

3.2 Methodology

As illustrated in Figure 2, the interpretation process is divided into two orthogonal pipelines. **1) Token back -racing**: The horizontal pipeline traces the path of tokens from the end to the start. Through causal back-tracing, tokens that are strongly correlated with a target token can be effectively identified, allowing us to focus on the most relevant information flows rather than exhaustively analyzing the dense connections across all tokens. This approach helps identify the key relationships between tokens, thereby pinpointing the crucial positions of key tokens in commonsense reasoning (as defined in §3.1). **2) Decode parametric concept or attribute**: The second pipeline, shown vertically, analyzes the patterns within LLMs when generating a specific token, including inner behaviors and activation characteristics. It explains the behavior of modules (e.g., residual blocks, Attention heads, and MLPs) by evaluating the information related to the target content (e.g., $\mathcal{A}_t$, $\mathcal{A}_f$, $\mathcal{O}_p$ and $\mathcal{O}_c$) within modules' output. Subsequently, it decodes the semantic information and patterns encoded in these modules into human-understandable formats.

Instantiation of tracing token-to-token path. We employ activation patching (Wang et al., 2023) as an effective tool for causal back-tracing. This

method originates from causal mediation analysis (Vig et al., 2020), where the results of direct effect enable us to identify the significant heads (the right side of Fig. 2). Heads with the Top-5 direct effect are considered contributors to generating a token. By examining the attention patterns in these important heads, the top 2 previous tokens with the highest attention scores are considered to be correlated with the current token and serve as the token to trace and analyze. This process can then be iteratively applied to discover the transition path across tokens. Activation patching relies on high-quality counterfactual data, which is paired with original data to calculate the direct effect for each head. It must be carefully designed to change specific semantics within a sentence minimally, without disrupting other narrative settings. We automatically generate this counterfactual data by GPT-4 (OpenAI, 2023) (see §A.1).

Instantiation of decoding parametric concept or attribute. We use logit attribution (nostalgebraist, 2021) to interpret the module behavior across layers. The method projects hidden states into the vocabulary space using the model's pretrained unembedding matrix and obtains its distribution on vocabulary space. Therefore, the method reveals the information contained in current hidden states and explains the contribution of specific heads or MLPs or residual blocks to the predicted token. Specifically, we calculate the softmax probability of the observed tokens ($\mathcal{O}_p$, $\mathcal{O}_c$, $\mathcal{A}_t$ or $\mathcal{A}_f$) after projection. The probabilities across layers will form the curves (see examples in Figure 3a), indicating the module's inner reasoning process.

To validate the interpreting results obtained by logit attribution, for MLP, we adopt Sparse Autoencoder (SAE) (Templeton et al., 2024) to decode the semantic information embedded in the parameters and activations. (e.g., Information related to "*magic*" is decoded in MLP of layer 8 when feeding "*Harry Potter*" to the model.) Based on dictionary learning, SAE translates the hidden states of LLMs into several interpretable pieces, or termed *features*. These features are activated on sparse token sequences with specific patterns, and most can be interpreted by GPT-4 (Lieberum et al., 2024) into concrete semantic descriptions. Regarding attention heads, we use probing to decode the semantic information. We project the outputs of the heads into the vocabulary space and examine the top-20 tokens in the head's output distribution to decode the semantic information. Furthermore, we applied knockout (Wang et al., 2023) to verify identified heads and MLPs. This method replaces the activations of modules with the average activation from counterfactual data. Analyzing changes in model performance allows us to validate the functional roles of these key components.

3.3 Application of Interpreting Results

Two methods are adopted to explore the application of interpreting results. **1) Selective supervised fine-tuning (SSFT)**: Zhang et al. (2024); Chen et al. (2024) proposed a method to enhance model's capability through updating a small set of parameters. We directly use the same settings without modification for effective verifications. Specifically, given a sequence of attention heads and MLPs ordered by their significance, denoted as $(MLP.l_1), (Head.l_2.h_2), (Head.l_3.h_3), \ldots$, where l_i represents the layer index and h_i represents the head index of the i^{th} ranked head, only top K heads and top M MLPs are exclusively updated during fine-tuning. We optimize both the corresponding input mapping matrix $\{W_{l_1}^{h_1}, W_{l_2}^{h_2}, ..., W_{l_K}^{h_K}\}$ and the output mapping matrix $\{O_{l_1}^{h_1}, O_{l_2}^{h_1}, ..., O_{l_K}^{h_K}\}$ in top K heads simultaneously. For the selected MLP layer, we update all parameters in this layer. **2) Representation engineering**, which adjusts the model's internal hidden states to influence its behavior, has proven to be an effective method for modulating model performance (Zou et al., 2023). Following the approach outlined in Xiao et al. (2024); Templeton et al. (2024), we correct the model's erroneous behavior using:

$$\tilde{\mathbf{h}}_l = \mathbf{h}_l + k\mathbf{x}_t, \quad (1)$$

where $\mathbf{h}_l$ represents the original output of residual block at layer l, $\mathbf{x}_t$ is the feature direction corresponding to the correct knowledge identified using SAE, k is the steering magnitude which we set 5.

4 Experiments

4.1 Experiments Overview

The experiment results are presented in a back-tracing manner. Consider a case from StrategyQA where the question is "*Q: Can Harry Potter book a flight on Asiana Airlines?*" and Gemma2-7B's output is "*Harry Potter is a fictional character. Fictional characters cannot book flights. Thus, Harry Potter cannot book a flight on Asiana Airlines. So*

the answer is no.". We begin decoding the parametric concept starting from $\mathcal{A}$ (i.e., "*no*"). By tracing back its proceeding tokens, we find it first passes through $\mathcal{C}$ (i.e., "*cannot*"), then transitions to $\mathcal{R}$ (i.e., "*Thus*"), and ultimately arrives at $\mathcal{O}$ (i.e., "*fictional*"). We term this process as **conclusion fusion and generation** (§4.2). Diving deeper into $\mathcal{O}$, our analysis of $\mathcal{O}_p$ illuminates the underlying mechanisms of **object retrieval and rerank** (§4.3). Further tracing the origin of $\mathcal{O}$ leads us to $\mathcal{S}$ (i.e., "*Harry Potter*"), uncovering the mechanisms of **subject augmentation and broadcast** (§4.4). We extend our investigation across different models and datasets in §4.5, and finally explore practical applications of these reasoning mechanisms through SSFT and representation engineering (§4.6).

Models We conducted experiments on two popular open-sourced models, Gemma2-9B (Team et al., 2024) and Llama2-7B (Touvron et al., 2023). The results in the Section 4 primarily focus on Gemma2-9B, as Sparse Autoencoders (SAEs) have been trained for all its layers (including residual and MLP layers) (Lieberum et al., 2024), enabling comprehensive validation of our analyses. See Appendix A.5 for results on Llama2-7B.

Datasets We selected three widely used commonsense reasoning benchmark datasets: **StrategyQA** (Geva et al., 2021a), **CommonsenseQA** (Talmor et al., 2018), and **SocialIQA** (Sap et al., 2019). These datasets focus on distinct dimensions of commonsense reasoning and see Tab. 13 and 14 for examples. The results are primarily reported on StrategyQA, with results for the other two datasets provided in §A.4. All metrics and curves are averaged over 100 samples. Prompts from Wei et al. (2022) and Li et al. (2024) are adopted to elicit model's reasoning abilities.

4.2 Conclusion Fusion and Generation

We start from decoding the information of $\mathcal{A}_t$ and $\mathcal{A}_f$ (i.e. "*yes*" and "*no*") in residual blocks, attention layers, and MLP layers at the position of predicting $\mathcal{A}$ as shown in Figure 3a. The curves of residual blocks depicts how the model predicts $\mathcal{A}$ across layers while curves of attention and MLP layers depict the module contribution to the $\mathcal{A}_t$ and $\mathcal{A}_f$. The prediction of $\mathcal{A}$ can be divided into three stages: (i) **Stage** 1 (layers $0-24$): Little to no answer-related information is present in residual blocks, attention and MLP layers, indicating the model is still processing the input. (ii) **Stage** 2 (layers $25-33$): Information related to the answer increases, yet the probabilities for $\mathcal{A}_t$ and $\mathcal{A}_f$ are close across residual blocks. Within the modules, attention heads begin to convey answer-related information from layer 25 and the MLP follows to encode this information from layer 26. Notably, the heads' outputs show similar information for both $\mathcal{A}_t$ and $\mathcal{A}_f$, but the MLPs' outputs assign a higher probability to $\mathcal{A}_t$. In this stage, the model start to generate an answer but has not yet identified the correct one. (iii) **Stage** 3: By layer 34, the model distinguishes the correct answer $\mathcal{A}_t$, with its probability sharply rising and the $\mathcal{A}_f$'s probability decreasing. At the same layer, the attention output sharply spikes for $\mathcal{A}_t$ (probability near 1.0), while the MLP output is much lower (around 0.1). Afterward, the outputs of MLPs further increase $\mathcal{A}_t$'s probability (layers $36-38$), leading to the final prediction. As a conclusion, attention head is responsible for the fusion of related information, while the MLP enhances the probability of the correct answer, contributing to the generation of the final answer.

We further investigated the semantic information encoded in the outputs of MLP and attention heads for verification. In attention heads, we found that in stage 2 and 3, the key heads encoded information related to both $\mathcal{A}_t$ and $\mathcal{A}_f$ (see the outputs of heads in Tab. 1). Meanwhile, numerous features related to decision-making (see Tab. 1) are identified in

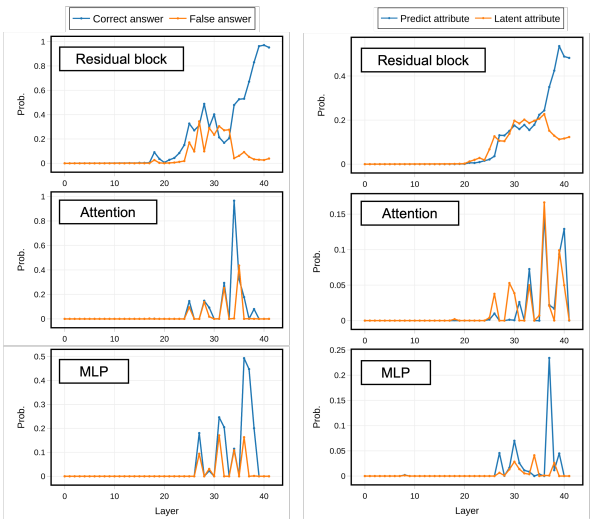

(a) (b)

Figure 3: (a) Logit attribution of $\mathcal{A}_t$ and $\mathcal{A}_f$ at predicting $\mathcal{A}$. (b) Logit attribution of $\mathcal{O}_p$ and $\mathcal{O}_l$ at predicting $\mathcal{O}$.

Head	Top tokens in projection
28.06	`yes, yeah, no, nil, Yes`
32.07	`Noah, node, Noah, no, Nora`
34.09	`denying, denied, denial, deny`
35.14	`ye, Ye, Yea, YE, yes, YES, Yeh`

Table 1: Top-scoring tokens in the key attention heads output when predicting $\mathcal{A}$.

Layer	ID	Feature Explanation
27	76551	questions and answers related to decision-making and assessments.
30	21336	affirmative and negative responses to questions.
38	101266	answers presented in a structured format, particularly in multiple-choice or quiz contexts.

Table 2: Top-scoring features decoded by SAE in the output of MLP when predicting $\mathcal{A}$.

MLPs. Furthermore, knocking out these key heads and MLPs significantly reduces the probability of $\mathcal{A}_t$ (see Fig. 19). These findings provide additional evidence supporting the critical role of the MLP and Attention layer in the answer generation process.

Finally, we applied activation patching to identify key heads and trace the information for generating $\mathcal{A}$. Tracing the information flow, the path began at the conclusion $\mathcal{S}$, progressed to the reasoning conjunctive adverb $\mathcal{R}$, and finally arrived at object $\mathcal{O}$. In the process, we discovered that $\mathcal{R}$ act as **anchors for the fusion and transport of conclusion-related information** in the reasoning process. For a detailed examination of the trace from $\mathcal{A}$ to $\mathcal{O}$, and an in-depth analysis of answer-related information at $\mathcal{R}$, refer to §A.3.

4.3 Object Retrieval and Rerank

The object information $\mathcal{O}$ decoded in the outputs of the residual block, attention layers and MLP layers are shown in Fig. 3b. We compare as many related objects, including the predicted object $\mathcal{O}_p$ and candidate object $\mathcal{O}_c$, as possible. For residual block, the object information emerges at around layer 26. However, $\mathcal{O}_p$ is not dominant in the first place, as the probabilities of $\mathcal{O}_p$ and $\mathcal{O}_c$ increase alternately. For attention heads, $\mathcal{O}_p$ and $\mathcal{O}_c$ interleave, with neither showing explicit dominance throughout the whole layers. On the contrary, MLP shows obvious preference on $\mathcal{O}_p$, where correct object information is prominent across almost all layers. Notably, at layer 37, $\mathcal{O}_p$ is clearly dominant, while $\mathcal{O}_c$ remains minimal. This sharp spike aligns with a key transition point in the curve of residual block. From these observations, it seems that 1) both $\mathcal{O}_p$ and $\mathcal{O}_c$ are integrated during the process of object token generation. 2) The attention heads initially retrieve the information for both $\mathcal{O}_p$ and $\mathcal{O}_c$, while MLPs subsequently rerank $\mathcal{O}_p$ to the top position.

To validate our finding, we knock out these key heads and MLPs, as shown in Fig. 19. The decreasing of probability of $\mathcal{O}_p$ reveals the important role of these modules. In addition, we also look into the output of heads and MLP. As shown in Tab. 10, attention heads encode a rich set of attribute information relevant to the subject (e.g., "*British*", "*wizard*", "*book*", and etc). Meanwhile, in Tab. 8, the decoded features by MLP are strongly related to "*identity and character*". It is high correlated to $\mathcal{O}_p$, but none of them is related to $\mathcal{O}_c$. These results validates the function of retrieving and reranking for attention head and MLP, respectively.

Finally, we utilize activation patching to identify the heads with causal effect (see Fig. 13a) and find these heads focus on two critical token positions, $\mathcal{S}$ and end of question. Therefore, we trace back to $\mathcal{S}$ to investigate the origin of $\mathcal{O}$.

4.4 Subject Augmentation and Broadcast

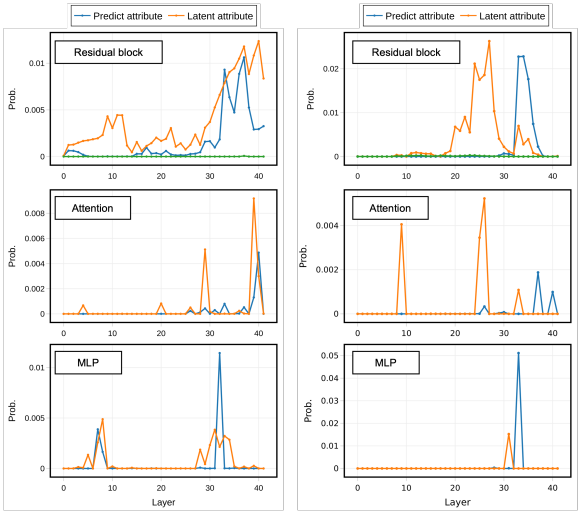

(a) (b)

Figure 4: (a) Logit attribution of $\mathcal{O}_p$ and $\mathcal{O}_l$ at $\mathcal{S}$. (b) Logit attribution of $\mathcal{O}_p$ and $\mathcal{O}_l$ at the end of question.

Generally, in commonsense reasoning datasets, the $\mathcal{S}$ always appears in both the question and the rationale. Through analysis, we observe that the $\mathcal{S}$ in the rationale can also be back-traced to the $\mathcal{S}$ in

the question. Therefore, we treat the position of $\mathcal{S}$ in the question as a focal point for deeper analysis.

Figure 4a illustrates the information of $\mathcal{O}_p$ and $\mathcal{O}_c$ decoded in the outputs. Notably, we observe that: 1) In residual block, it contains obvious information regarding both $\mathcal{O}_p$ and $\mathcal{O}_c$ across various layers, with $\mathcal{O}_c$ being more prominent at the end. 2) another two curves show that both attention heads and MLPs have a large influence on $\mathcal{O}_p$ and $\mathcal{O}_c$. To further decode information, we identifies that MLPs in layers 7 and 32 encode abundant features related to $\mathcal{O}$ (see Tab. 9). Meanwhile, Probing also reveals that heads in layers 29 and 39 rank the $\mathcal{O}_c$ at top. In addition to diminishing the impact of the information from any previous token, we also examine the three corresponding curves at the position before $\mathcal{S}$ (for instance, "Question: **Can** Harry Potter"). The results (green line in Fig. 4a) reveal that the information regarding $\mathcal{O}$ is virtually zero. It indicates that the emergence of $\mathcal{O}_p$ and $\mathcal{O}_l$ is indeed contingent upon the appearance of $\mathcal{C}$ and is independent of any previous tokens. In conclusion, both the MLP and heads play essential roles in assisting the model to associate and extend from $\mathcal{S}$ to related $\mathcal{O}_p$ and $\mathcal{O}_l$. We refer to this stage, along with the contributions of the MLP and heads, as **subject augmentation**.

Regarding the question's end token position, Fig. 4b also presents the three corresponding curves. (1) In the residual, both $\mathcal{O}_p$ and $\mathcal{O}_l$ appear across multiple layers. On the contrary to concept token position, $\mathcal{O}_p$ has a greater presence than $\mathcal{O}_l$. (2) The curves for the MLP and heads also encapsulate information about both $\mathcal{O}_p$ and $\mathcal{O}_l$, and further enhance the importance of $\mathcal{O}_p$. These observations indicate that even at seemingly unrelated token positions, the $\mathcal{O}$ corresponding to the $\mathcal{S}$ (or the knowledge they encompass) can be broadcast. The original order of $\mathcal{O}$ may be broadcast based on the current context, ultimately influencing the generation of $\mathcal{O}_p$. We term this stage as **subject broadcasting**.

4.5 Generalization of findings

We further analyzed the reasoning process of Gemma2-9B on CommonsenseQA and SocialIQA. The results (see §A.4) indicate that the reasoning process on these two datasets also consists of object retrieval and reranking as well as conclusion fusion and generation. However, the phenomenon of subject augmentation was not prominently observed in the SocialIQA and CommonsenseQA datasets. We hypothesize that this is due to the explicit provision of the required factual knowledge within the question context, which diminishes the model's need to infer additional related facts. In addition, we validated the proposed reasoning process on the Llama2-7B model across three datasets, and similar results are observed on this model. Detailed results can be found in§A.5.

Models	ID Task	OOD Task		
	Strategy	CSQA	SIQA	Wino
Gemma2-9B	70.7	75.7	73.0	61.2
+ SFT (9B)	79.0	74.3	70.9	60.3
+ SSFT (0.3B)	80.3	76.2	74.0	65.2
Llama2-7B	62.5	68.3	67.9	55.5
+ SFT (7B)	77.3	54.8	59.0	52.7
+ SSFT (0.2B)	78.5	64.1	63.2	61.1

Table 3: Results on four commonsense reasoning tasks (i.e., StrategyQA, CSQA, Winogrande, and SocialIQA) before and after tuning on the StrategyQA dataset using SFT and SSFT.

4.6 Application of Interpreting Results

Failure Case Analysis. Our analysis of Gemma2-7B's incorrect responses on StrategyQA reveals four error types (Fig. 5): 1) Reference Errors: retrieving irrelevant or incorrect attributes; 2) Logic Errors: insufficient knowledge to support conclusions; 3) Conclusion Errors: wrong answers despite correct reasoning; and 4) Concept Errors: misidentification of target concepts to analyze. Reference Errors dominate at 74% of all cases. Further probing reveals that these errors primarily stem from reranking issues rather than knowledge gaps, as correct objects typically appear within the model's top-5 predicted tokens. Following Zhang et al. (2024) and Chen et al. (2024), we propose enhancing commonsense reasoning by targeted training of specific MLP and Attention heads involved in these tasks.

Experiment Setup. With the key Attention heads and MLPs identified for generating attributes, we conduct the selective supervised fine-tuning (SSFT) experiment on StrategyQA task by only updating the parameters of selected heads and MLPs. Specifically, Following (Fu et al., 2023) and (Huang et al., 2022), each sample in our training data is organized with the format of "`{Few-shot CoT prompt} Q: {Question}. A: {Rationale}`". Considering the generalization, we introduce another commonsense reasoning test dataset, WinoGrande (Sakaguchi et al., 2021).

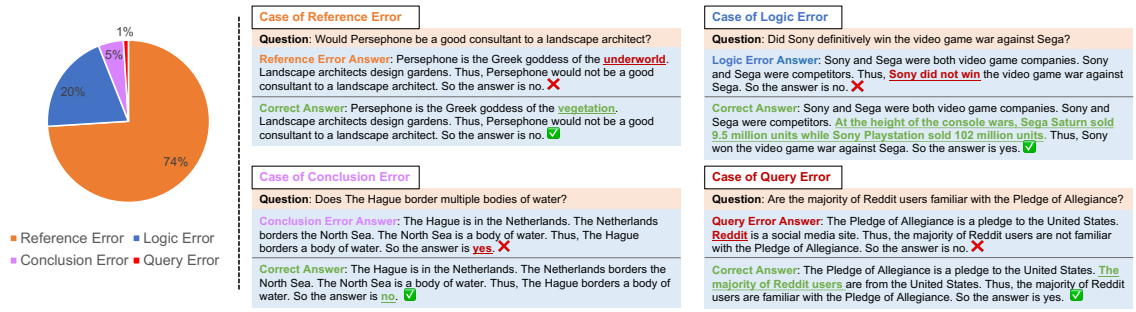

Figure 5: The distribution of the four types of errors encountered by Gemma2-7B on StrategyQA. 1) Reference Error: The model retrieves irrelevant or wrong attributes. 2) Logic Error: incomplete reasoning steps. 3) Conclusion Error: reaches an incorrect answer but based on correct rationale. 4) Concept Error: incorrectly identifies the target concept for analysis. We use GPT-4 to automatically classify the failure types and see Fig. 21 for the prompt.

We selectively fine-tune the top 32 Attention heads (for knowledge retrieval) and top 1 MLP layers (for knowledge reranking) with a learning rate of 1×10^{-4} and a batch size of 32 for 2 epochs. For supervised fine-tuning, a learning rate of 1×10^{-5} is utilized, while all other configurations remain consistent with SSFT training. Experiments are conducted on 8 NVIDIA A100 (80GB) GPUs.

Experiment Results. The comparative results between SSFT and SFT are presented in Table 3. For the experiments of Gemma2-9B on StrategyQA, both SSFT and SFT improved performance, achieving gains of $+8.3\%$ and $+9.6\%$, respectively. While SFT shows a comparable enhancement for the StrategyQA task, it adversely affected performance on OOD tasks, with an average decrease of -1.5%. In contrast, SSFT continued to bolster the model's reasoning ability across all OOD commonsense reasoning tasks, improving the performance by an average of $+2.6\%$. These findings suggest that selectively fine-tuning a small fraction of key components for commonsense reasoning can boost performance on ID tasks while maintaining generalizability, highlighting the effectiveness of our previous exploration. A similar trend was observed in the Llama2-7B results. Through mechanism analysis of the model before and after SSFT, we further validate that SSFT enhances the model's knowledge retrieval and reranking capabilities. (See Fig. 20). Additionally, we further validate the effectiveness of SSFT through training on two other datasets (Tab. 11 and 12).

Representation engineering results. We also utilize representation engineering to correct the model's (Gemma2-9B) reasoning process on the question, e.g., "*Would Persephone be a suitable consultant to a landscape architect?*". The model initially defaults to identifying "*Persephone as the Greek goddess of the underworld*", leading to an incorrect assessment. The correct reference is "*Persephone is the Greek goddess of spring*". By introducing feature directions related to deities or nature into the residual block at layer 37(object retrieval), we strengthened the model's tendency to associate Persephone with spring. This tendency can largely contribute to the correct answer, and rectify the model's response. As a result, 93% failure cases can be rectified, illustrating the rationality of the identified interpreting results.

5 Conclusion

In conclusion, our research sheds light on the intricate dynamics of commonsense reasoning within LLMs, revealing a structured process that parallels human cognitive reasoning. By meticulously analyzing the hidden states across various transformer layers and token positions, we identified a multi-faceted mechanism that integrates knowledge augmentation, retrieval, and answer generation—essentially resembling a retrieval-augmented generation framework. Our findings underscore the pivotal roles played by both attention heads and MLPs in the manifestation of factual knowledge, highlighting a dual approach to knowledge processing. Furthermore, our experiments demonstrated that while LLMs often possess relevant factual knowledge, they frequently struggle to retrieve the correct information during inference. Through selective fine-tuning of key components, we achieved notable enhancements in reasoning performance across diverse contexts, indicating that targeted adjustments can effectively optimize the reasoning capabilities of LLMs.

6 Limitations

While the methods and findings presented in this study provide valuable insights into the internal mechanisms of large language models (LLMs), there are several limitations:

Scope of Evaluation: The experiments primarily focus on commonsense reasoning tasks, and the results may not fully generalize to other types of reasoning or NLP tasks. Future work could extend the methodology to explore how these internal mechanisms behave across a wider range of tasks.

Model Dependency: Our analysis is based on the specific architectures and pretrained models used in this study. While the interpretability tools such as logit attribution, activation patching, and sparse autoencoders provide useful insights, the observed behaviors may vary with different models or architectures. The findings may be influenced by the particular training data and the design choices of the models.

Complexity of Causal Back-Tracing: The causal back-tracing method, while effective in identifying key tokens and correlations, remains computationally expensive and may require further optimization for large-scale models. Additionally, accurately interpreting causal relationships in highly complex networks like transformers is a non-trivial task and may be subject to noise or inaccuracies, especially in deep layers.

Interpretability Limitations: While we provide insights into model behavior by examining attention heads, MLPs, and other components, the level of interpretability remains limited. Fully understanding the underlying reasons for model decisions, especially in tasks involving nuanced or implicit commonsense knowledge, may still be out of reach with current methods.

Human Evaluation: While the interpretability tools offer a mechanistic view of the model, the final conclusions and explanations are still subject to human interpretation. There is a risk of oversimplification or misinterpretation when mapping complex internal mechanisms to human-understandable explanations, particularly in highly abstract or nonlinear decision-making processes.

References

Nora Belrose, Zach Furman, Logan Smith, and et al. 2023. Eliciting latent predictions from transformers with the tuned lens. *CoRR*, abs/2303.08112.

Lukas Berglund, Meg Tong, Maximilian Kaufmann, Mikita Balesni, Asa Cooper Stickland, Tomasz Korbak, and Owain Evans. 2023. The reversal curse: Llms trained on "a is b" fail to learn "b is a". In *The Twelfth International Conference on Learning Representations*.

Trenton Bricken, Adly Templeton, Joshua Batson, Brian Chen, Adam Jermyn, Tom Conerly, Nick Turner, Cem Anil, Carson Denison, Amanda Askell, Robert Lasenby, Yifan Wu, Shauna Kravec, Nicholas Schiefer, Tim Maxwell, Nicholas Joseph, Zac Hatfield-Dodds, Alex Tamkin, Karina Nguyen, Brayden McLean, Josiah E Burke, Tristan Hume, Shan Carter, Tom Henighan, and Christopher Olah. 2023. Towards monosemanticity: Decomposing language models with dictionary learning. *Transformer Circuits Thread*. Https://transformer-circuits.pub/2023/monosemantic-features/index.html.

Wei Chen, Zhen Huang, Liang Xie, Binbin Lin, Houqiang Li, Le Lu, Xinmei Tian, Deng Cai, Yonggang Zhang, Wenxiao Wan, et al. 2024. From yes-men to truth-tellers: Addressing sycophancy in large language models with pinpoint tuning. *arXiv preprint arXiv:2409.01658*.

Arthur Conmy, Augustine Mavor-Parker, Aengus Lynch, Stefan Heimersheim, and Adrià Garriga-Alonso. 2023. Towards automated circuit discovery for mechanistic interpretability. In *Advances in Neural Information Processing Systems*, volume 36, pages 16318–16352. Curran Associates, Inc.

Damai Dai, Li Dong, Yaru Hao, Zhifang Sui, Baobao Chang, and Furu Wei. 2022. Knowledge neurons in pretrained transformers. In *Proceedings of the 60th Annual Meeting of the Association for Computational Linguistics (Volume 1: Long Papers)*, pages 8493–8502, Dublin, Ireland. Association for Computational Linguistics.

Guy Dar, Mor Geva, Ankit Gupta, and et al. 2023. Analyzing transformers in embedding space. In *ACL*, pages 16124–16170. Association for Computational Linguistics.

Subhabrata Dutta, Joykirat Singh, Soumen Chakrabarti, and Tanmoy Chakraborty. 2024. How to think step-by-step: A mechanistic understanding of chain-of-thought reasoning. *ArXiv*, abs/2402.18312.

Yao Fu, Hao Peng, Litu Ou, Ashish Sabharwal, and Tushar Khot. 2023. Specializing smaller language models towards multi-step reasoning. In *International Conference on Machine Learning*, pages 10421–10430. PMLR.

Leo Gao, Tom Dupré la Tour, Henk Tillman, Gabriel Goh, Rajan Troll, Alec Radford, Ilya Sutskever, Jan Leike, and Jeffrey Wu. 2024. Scaling and evaluating sparse autoencoders. *arXiv preprint arXiv:2406.04093*.

Mor Geva, Jasmijn Bastings, Katja Filippova, and Amir Globerson. 2023. Dissecting recall of factual associations in auto-regressive language models. In *Proceedings of the 2023 Conference on Empirical Methods in Natural Language Processing*, pages 12216–12235, Singapore. Association for Computational Linguistics.

Mor Geva, Avi Caciularu, Kevin Ro Wang, and et al. 2022. Transformer feed-forward layers build predictions by promoting concepts in the vocabulary space. In *EMNLP*, pages 30–45. Association for Computational Linguistics.

Mor Geva, Daniel Khashabi, Elad Segal, Tushar Khot, Dan Roth, and Jonathan Berant. 2021a. Did aristotle use a laptop? a question answering benchmark with implicit reasoning strategies. *Transactions of the Association for Computational Linguistics*, 9:346–361.

Mor Geva, Roei Schuster, Jonathan Berant, and et al. 2021b. Transformer feed-forward layers are key-value memories. In *EMNLP*, pages 5484–5495. Association for Computational Linguistics.

Nicholas Goldowsky-Dill, Chris MacLeod, Lucas Sato, and Aryaman Arora. 2023. Localizing model behavior with path patching. *arXiv preprint arXiv:2304.05969*.

Michael Hanna, Ollie Liu, and Alexandre Variengien. 2023. How does gpt-2 compute greater-than?: Interpreting mathematical abilities in a pre-trained language model. *arXiv preprint arXiv:2305.00586*.

Yifan Hou, Jiaoda Li, Yu Fei, Alessandro Stolfo, Wangchunshu Zhou, Guangtao Zeng, Antoine Bosselut, and Mrinmaya Sachan. 2023. Towards a mechanistic interpretation of multi-step reasoning capabilities of language models. In *Proceedings of the 2023 Conference on Empirical Methods in Natural Language Processing*, pages 4902–4919, Singapore. Association for Computational Linguistics.

Jiaxin Huang, Shixiang Shane Gu, Le Hou, Yuexin Wu, Xuezhi Wang, Hongkun Yu, and Jiawei Han. 2022. Large language models can self-improve. *arXiv preprint arXiv:2210.11610*.

Stefanie Krause and Frieder Stolzenburg. 2023. Commonsense reasoning and explainable artificial intelligence using large language models. In *European Conference on Artificial Intelligence*, pages 302–319. Springer.

Jiachun Li, Pengfei Cao, Chenhao Wang, Zhuoran Jin, Yubo Chen, Daojian Zeng, Kang Liu, and Jun Zhao. 2024. Focus on your question! interpreting and mitigating toxic CoT problems in commonsense reasoning. In *Proceedings of the 62nd Annual Meeting of the Association for Computational Linguistics (Volume 1: Long Papers)*, pages 9206–9230, Bangkok, Thailand. Association for Computational Linguistics.

Tom Lieberum, Matthew Rahtz, J'anos Kram'ar, G. Irving, Rohin Shah, and Vladimir Mikulik. 2023. Does circuit analysis interpretability scale? evidence from multiple choice capabilities in chinchilla. *ArXiv*, abs/2307.09458.

Tom Lieberum, Senthooran Rajamanoharan, Arthur Conmy, Lewis Smith, Nicolas Sonnerat, Vikrant Varma, János Kramár, Anca Dragan, Rohin Shah, and Neel Nanda. 2024. Gemma scope: Open sparse autoencoders everywhere all at once on gemma 2. *arXiv preprint arXiv:2408.05147*.

Kevin Meng, David Bau, Alex Andonian, and Yonatan Belinkov. 2022. Locating and editing factual associations in gpt. In *Neural Information Processing Systems*.

nostalgebraist. 2021. Interpreting gpt: The logit lens.

OpenAI. 2023. Gpt-4 technical report.

Francesco Ortu, Zhijing Jin, Diego Doimo, Mrinmaya Sachan, Alberto Cazzaniga, and Bernhard Schölkopf. 2024. Competition of mechanisms: Tracing how language models handle facts and counterfactuals. In *Proceedings of the 62nd Annual Meeting of the Association for Computational Linguistics (Volume 1: Long Papers)*, pages 8420–8436, Bangkok, Thailand. Association for Computational Linguistics.

Keisuke Sakaguchi, Ronan Le Bras, Chandra Bhagavatula, and Yejin Choi. 2021. Winogrande: An adversarial winograd schema challenge at scale. *Communications of the ACM*, 64(9):99–106.

Maarten Sap, Hannah Rashkin, Derek Chen, Ronan LeBras, and Yejin Choi. 2019. Socialiqa: Commonsense reasoning about social interactions. *arXiv preprint arXiv:1904.09728*.

Robyn Speer, Joshua Chin, and Catherine Havasi. 2017. Conceptnet 5.5: An open multilingual graph of general knowledge. In *Proceedings of the AAAI conference on artificial intelligence*, volume 31.

Alon Talmor, Jonathan Herzig, Nicholas Lourie, and Jonathan Berant. 2018. Commonsenseqa: A question answering challenge targeting commonsense knowledge. *arXiv preprint arXiv:1811.00937*.

Gemma Team, Morgane Riviere, Shreya Pathak, Pier Giuseppe Sessa, Cassidy Hardin, Surya Bhupatiraju, Léonard Hussenot, Thomas Mesnard, Bobak Shahriari, Alexandre Ramé, et al. 2024. Gemma 2: Improving open language models at a practical size. *arXiv preprint arXiv:2408.00118*.

Adly Templeton, Tom Conerly, Jonathan Marcus, Jack Lindsey, Trenton Bricken, Brian Chen, Adam Pearce, Craig Citro, Emmanuel Ameisen, Andy Jones, Hoagy Cunningham, Nicholas L Turner, Callum McDougall, Monte MacDiarmid, C. Daniel Freeman, Theodore R. Sumers, Edward Rees, Joshua Batson, Adam Jermyn, Shan Carter, Chris Olah, and Tom Henighan. 2024. Scaling monosemanticity: Extracting interpretable

features from claude 3 sonnet. *Transformer Circuits Thread*.

Hugo Touvron, Louis Martin, Kevin Stone, Peter Albert, Amjad Almahairi, Yasmine Babaei, Nikolay Bashlykov, Soumya Batra, Prajjwal Bhargava, Shruti Bhosale, et al. 2023. Llama 2: Open foundation and fine-tuned chat models. *arXiv preprint arXiv:2307.09288*.

Jesse Vig, Sebastian Gehrmann, Yonatan Belinkov, Sharon Qian, Daniel Nevo, Yaron Singer, and Stuart M. Shieber. 2020. Investigating gender bias in language models using causal mediation analysis. In *NeurIPS*.

Kevin Ro Wang, Alexandre Variengien, Arthur Conmy, and et al. 2023. Interpretability in the wild: a circuit for indirect object identification in GPT-2 small. In *ICLR*.

Yifei Wang, Yuheng Chen, Wanting Wen, Yu Sheng, Linjing Li, and Daniel Dajun Zeng. 2024. Unveiling factual recall behaviors of large language models through knowledge neurons. In *Proceedings of the 2024 Conference on Empirical Methods in Natural Language Processing*, pages 7388–7402, Miami, Florida, USA. Association for Computational Linguistics.

Jason Wei, Xuezhi Wang, Dale Schuurmans, Maarten Bosma, Fei Xia, Ed Chi, Quoc V Le, Denny Zhou, et al. 2022. Chain-of-thought prompting elicits reasoning in large language models. *Advances in Neural Information Processing Systems*, 35:24824–24837.

Yuxin Xiao, Chaoqun Wan, Yonggang Zhang, Wenxiao Wang, Binbin Lin, Xiaofei He, Xu Shen, and Jieping Ye. 2024. Enhancing multiple dimensions of trustworthiness in llms via sparse activation control. In *The Thirty-eighth Annual Conference on Neural Information Processing Systems*.

Jian Xie, Kai Zhang, Jiangjie Chen, Renze Lou, and Yu Su. 2024. Adaptive chameleon or stubborn sloth: Revealing the behavior of large language models in knowledge conflicts. In *The Twelfth International Conference on Learning Representations*.

Lei Yu, Meng Cao, Jackie CK Cheung, and Yue Dong. 2024. Mechanistic understanding and mitigation of language model non-factual hallucinations. In *Findings of the Association for Computational Linguistics: EMNLP 2024*, pages 7943–7956, Miami, Florida, USA. Association for Computational Linguistics.

Qinan Yu, Jack Merullo, and Ellie Pavlick. 2023. Characterizing mechanisms for factual recall in language models. In *Proceedings of the 2023 Conference on Empirical Methods in Natural Language Processing*, pages 9924–9959.

Zeping Yu and Sophia Ananiadou. 2024. Neuron-level knowledge attribution in large language models. In *Proceedings of the 2024 Conference on Empirical Methods in Natural Language Processing*, pages 3267–3280, Miami, Florida, USA. Association for Computational Linguistics.

Wei Zhang, Chaoqun Wan, Yonggang Zhang, Yiu-ming Cheung, Xinmei Tian, Xu Shen, and Jieping Ye. 2024. Interpreting and improving large language models in arithmetic calculation. *arXiv preprint arXiv:2409.01659*.

Xuhui Zhou, Yue Zhang, Leyang Cui, and Dandan Huang. 2020. Evaluating commonsense in pre-trained language models. In *Proceedings of the AAAI conference on artificial intelligence*, volume 34, pages 9733–9740.

Andy Zou, Long Phan, Sarah Chen, James Campbell, Phillip Guo, Richard Ren, Alexander Pan, Xuwang Yin, Mantas Mazeika, Ann-Kathrin Dombrowski, et al. 2023. Representation engineering: A top-down approach to ai transparency. *arXiv preprint arXiv:2310.01405*.

A Appendix

A.1 Activation patching details

Counterfactual data generation We use GPT-4 to assist in automatically generating the counterfactual data required for activation patching, with the prompt shown in Figure 6 and an example in Table 5. Additionally, we implement a post-processing step: if the predicted token for the counterfactual data matches the prediction for the data under investigation (which would fail to perturb the model's behavior), GPT-4 is prompted to regenerate the counterfactual data.

We conduct experiments to compare the performance of "GPT-4" and "human". we engaged ten master's students specializing in Natural Language Processing as volunteers. Five students were manually executing all procedures, including generating X_c, analyzing key component behaviors, and developing data templates. The remaining students then compared their annotations with those generated by GPT-4 to judge which more accurately represented the component behavior. Overall, the results (Table 4) demonstrate that GPT-4 is highly accepted by human evaluators, with the combination of "GPT wins" and "Ties" exceeding 80%, underscoring its robust reliability. These indicate that *GPT-4's outputs are almost consistent with those generated by humans.*

Activation patching metric We use the rate of change in the probability of the predicted token before and after perturbation as the metric for path patching.

Table 4: Comparison of differences between GPT-4 and human annotations

GPT-4 Wins	Human Wins	Ties
8%	12%	80%

A.2 Dataset details

A.3 Details of tracing from answer $\mathcal{A}$ to object $\mathcal{O}$

We found that the attention heads responsible for generating $\mathcal{A}$ primarily focus on the conclusion token $\mathcal{C}$, as demonstrated by the pattern of head 25.08 in Tab. 6. Therefore, we traced back to the $\mathcal{C}$, Fig. 7a shows the probabilities of $\mathcal{A}_t$ and $\mathcal{A}_f$ in the residual block, attention, and MLP outputs at the conclusion token position. It is evident that the model distinguishes the correct answer $\mathcal{A}_t$ in the deep layers, with both the attention and MLP outputs containing substantial information related to $\mathcal{A}_t$.

Next, we identified the heads for generating $\mathcal{C}$ using activation patching and discovered that the key attention heads primarily focus on the reasoning conjunctive adverb $\mathcal{R}$ (i.e., "*Thus*" in head 31.03 pattern in Tab. 6). We also observed that the attention head outputs contain information related to the correct answer $\mathcal{A}_t$, such as "*yes*," "*indeed,*" and "*true.*" Based on these findings, we conducted further probing at $\mathcal{R}$ to trace the origin of $\mathcal{A}_t$.

Through decoding information of $\mathcal{A}_t$ and $\mathcal{A}_f$ at $\mathcal{R}$ (Fig. 7b), we find that deep layers $(30-34)$ already encode rich information related to the correct answer $\mathcal{A}_t$. To trace the origin of the answer-related information, we employed a modified activation patching to identify the key Attention heads. Specifically, we iteratively corrupted the output of each attention head from layer $0-30$ using the activation in counterfactual data, then identified the key attention heads that have a significant negative influence on the probability of $\mathcal{A}_t$ in residual block (layer 30) output. Three key Attention heads (25.7, 25.8 and 25.9) are identified that primarily focus on the position of attribute $\mathcal{A}$ (e.g., "company"). From the observation above, we conclude a key finding: *reasoning conjunctive adverbs serve as an anchor for gathering and transferring conclusion-related information in reasoning process*. Therefore, our investigation continuously traces back to the position of object $\mathcal{O}$ prediction.

A.4 Results on CommonsenseQA and SocialIQA

We further apply our interpreting method to CommonsenseQA (Talmor et al., 2018) and SocialIQA (Sap et al., 2019) and find the model's reasoning process within these two datasets consists of **attribute retrieval**, **attribute rerank**, and **answer generation** as shown in Fig. 8. Similarly, we start by decoding the probability of $\mathcal{A}_t$ and $\mathcal{A}_f$ at the position of predicting answer $\mathcal{A}_t$. The decoding curve of CommonsenseQA is in Fig 10b and SocialIQA result is in Fig 12b. It is observed that the information trend in residual block, Attention, and MLP is similar across the two datasets. Specifically, the probability of $\mathcal{A}_t$ increases significantly at layer 30, while Attention output encodes $\mathcal{A}_t$ related information before layer 30 and $\mathcal{A}_t$ relate information emerges in MLP at layer around 32. Therefore, we

Prompt Template for Counterfactual Data Generation

```
<Inputs><topic> The particular topic being studied</topic>
<input_sentence> The original sentence provided for analysis</input_sentence>
<predicted_content> The specific words reflecting model behavior</predicted_content>
<first_word_predicted> The first word initially predicted by the model</first_word_predicted></Inputs>

<Instructions Structure>
1. Instruct the assistant to begin by analyzing the original input sentence and why it leads to the specific predicted word.
2. Guide the assistant to think about changes that could alter the model's prediction.
3. Instruct the assistant to provide the reason for the model's original prediction.
4. Request the assistant to modify the original sentence so that the model's prediction changes.
5. Instruct the assistant to explain the modification's rationale, focusing on why the modified sentence now influences a different predicted outcome.
6. Ensure the output is formatted in the specified JSON structure.
</Instructions Structure>

<Instructions>
Your task is to analyze and modify a sentence to influence the predictive behavior of a language model. You will be given a topic, an input sentence,
the specific words predicted by the model, and the model's first predicted word.

Here is the topic and input sentence to modify: <topic>{$TOPIC}</topic> <input_sentence>{$INPUT_SENTENCE}</input_sentence>

Here are the words generated by model given the input sentence: <predicted_content>{$PREDICTED_CONTENT}</predicted_content>

Here is the first predicted word:
<first_word_predicted>{$FIRST_WORD_PREDICTED}</first_word_predicted>

Follow these steps carefully to complete the task:

1. **Analyze the Original Prediction**: Start by understanding the **input sentence** and why it leads the model to predict the
   **first_word_predicted** as the output under the specific **topic**. Consider the context, tone, or structure of the sentence that prompts this
    specific word choice by the model.
2. **Plan the Modification**: Think about how you could change the **input_sentence** minimally (by changing only 3-4 words) to alter the
   model's behavior so that it no longer predicts the original word or instead predicts a word with an opposite meaning. It's acceptable to change some
    of the sentence's meaning if it helps influence the output.
3. **Provide Analysis and Modification**:
   - Write the **reason for the original prediction** based on your analysis in Step 1.
   - Rewrite the **input_sentence** in a modified form that will change or flip the model's predicted word.
   - Explain your **reason for the modification**, focusing on how the changes you made will influence the model to predict a different word.

4. **Output the Final Result**: Format your response in JSON, as shown below:

```json
{
    "Reason for original prediction": "Explain why the original input caused the model to predict the initial word.",
    "Modified input": "Write the modified sentence here.",
    "Reason for modification": "Explain why the modified input will lead to a different prediction from the model."
}
```
Make sure each section is clear and precise. End your response with this JSON structure.
</Instructions>
```

Figure 6: Prompt for using GPT-4 to generate counterfactual data in activation patching.

conclude the answer generation process as follows: attention is responsible for copying and generating $\mathcal{A}_t$ related information and MLP is responsible for augmenting this information. Through backtracing, we identified the key heads for generating the correct answer (see key head distribution in Fig 9b and 11b). As shown in Tab. 7, we find the head output encodes rich information related to the correct answer and mainly attends to the object in rationale and choices in question. Therefore, we first trace back to the position of $\mathcal{C}$.

Since both datasets are in the form of multiple-choice questions, the answer (object) is already provided as one of the options. Therefore, we treat the correct answer as the predicted object $\mathcal{O}_p$ and the other options as candidate objects $\mathcal{O}_c$. The logit attribution curves for $\mathcal{A}_t$ and $\mathcal{A}_f$ are shown in Fig 10a and 12a for CommonsenseQA and SocialIQA respectively. As shown in the figure, the attention output contains both $\mathcal{O}_p$ and $\mathcal{O}_c$, while the MLP output only contains the $\mathcal{O}_p$. This finding aligns with our previous discovery on StrategyQA regarding the **object retrieval and reranking** mechanism: attention heads first aggregate all relevant objects, and then the MLP ranks these objects based on their relevance, selecting the $\mathcal{O}_p$ for the final output. These results further validate the generalizability of our approach and findings.

Finally, we used activation patching to identify the key attention heads responsible for generating $\mathcal{O}_p$. The distribution of important heads is shown in Fig. 9a and 11a. We found that the key heads primarily focus on the options in the question (see head pattern of 34.14 in Tab. 7), which serve as the source for all objects. With this, the complete reasoning process is concluded.

Table 5: Example of probing data X_r and counterfactual data X_c generated by GPT-4. Counterfactual data change the model (Gemma2-9B) prediction behavior by applying minimal change to the probing data.

Data	Model Input	Model Predict
X_r	Question: Kendall opened their mouth to speak and what came out shocked everyone. How would you describe Kendall? (1) a very quiet person (2) a very passive person (3) a very aggressive and talkative person Answer: Kendall opened their mouth to speak and what came out shocked everyone. Thus, Kendall is a very __	aggressive
X_c	Question: Kendall opened their mouth to speak and what came out **was softer than expected**. How would you describe Kendall? (1) a very quiet person (2) a very passive person (3) a very aggressive and talkative person Answer: Kendall opened their mouth to speak and what came out **was softer than expected**. Thus, Kendall is a very __	quiet

Pos.	Head	Attention score	Projection
$\mathcal{O}$	25.02	Q: Is Canon Inc. a Kabushiki gaisha?<newline> A: Canon Inc. is a	Japan, Japanese, Jepang, Japón, japan, Tokyo
$\mathcal{R}$	25.08	Q: Is Canon Inc. a Kabushiki gaisha?<newline> A: Canon Inc. is a Japanese company. Japanese companies are Kabushiki gaisha. Thus	confirmation, confirmación, Personendaten, verification
$\mathcal{S}$	31.03	Q: Is Canon Inc. a Kabushiki gaisha?<newline> A: Canon Inc. is a Japanese company. Japanese companies are Kabushiki gaisha. Thus, Canon Inc. is	yes, Yes, indeed
$\mathcal{A}$	25.08	Q: Is Canon Inc. a Kabushiki gaisha?<newline> A: Canon Inc. is a Japanese company. Japanese companies are Kabushiki gaisha. Thus, Canon Inc. is a Kabushiki gaisha. So the answer is	YES, true, Indeed confirmation, confirmación, confirmer, verification

Table 6: Attention score of the key attention heads (on StrategyQA in Gemma2-9B) on different tokens and top-k tokens after projecting the output of heads into the vocabulary space. The attention heads are obtained according to the activation patching result in Figure 13. The term Head 25.02 denotes the 2nd head in the attention layer of the 25th layer of the model.

A.5 Experiment results on Llama2-7B

On Llama2-7B, we apply the same method to interpret the reasoning process in StrategyQA (see Fig. 14, CommonsenseQA (Fig. 17) and SocialIQA (Fig. 12. Three phases of reasoning, i.e. **subject augmentation and broadcast**, **object retrieval and rerank**, **conclusion fusion and generation** are observed on StrategyQA. Similarly, **object retrieval and rerank** and **conclusion generation** are observed on CommonsenseQA and SocialIQA.

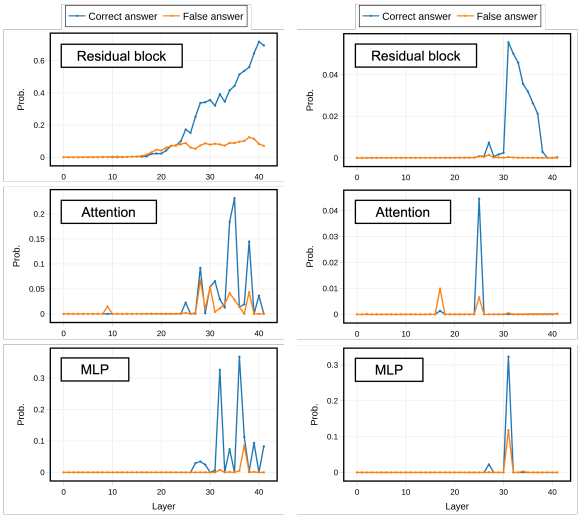

(a) (b)

Figure 7: Logit attribution results on StrategyQA of Gemma2-9B. (a) Probability of $\mathcal{A}_t$ and $\mathcal{A}_f$ when predicting $\mathcal{C}$. (b) Probability of $\mathcal{A}_t$ and $\mathcal{A}_f$ when at $\mathcal{R}$.

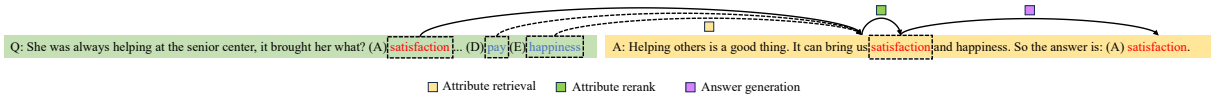

Figure 8: Model inner reasoning process on CommonsenseQA.

Pos.	Head	Attention score	Projection
$\mathcal{O}$	34.14	<newline>Question: A crane uses many a steel cable when working a what?<newline> (A) abaft (B) ship (C) winch (D) construction site (E) building<newline> Answer: A crane is a machine that is used to lift and move heavy objects. It is usually used in	construction, Konstruktion, autorytatywna, Construction
$\mathcal{A}$	31.15	<newline>Question: A crane uses many a steel cable when working a what?<newline> (A) abaft (B) ship (C) winch (D) construction site (E) building<newline> Answer: A crane is a machine that is used to lift and move heavy objects. It is usually used in construction sites. So the answer is: (D)	construction, constructions, struction, traction, construcción

Table 7: Attention score of the key attention heads (on CommonsenseQA in Gemma2-9B) on different tokens and top-k tokens after projecting the output of heads into the vocabulary space. The attention heads are obtained according to the activation patching result in Figure 9. The term Head 34.14 denotes the 14nd head in the attention layer of the 34th layer of the model.

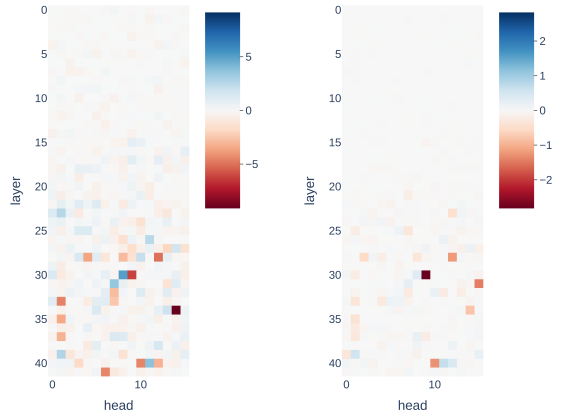

(a) Trace back at $\mathcal{A}$ (to $\mathcal{O}$) (b) Trace back at $\mathcal{O}$ (to choices)

Figure 9: Distribution of key heads (Gemma2-9B) during tracing back at different token positions on CommonsenseQA (averaged on 100 samples). The red squares indicate heads that have a significant positive impact on predicting the output token.

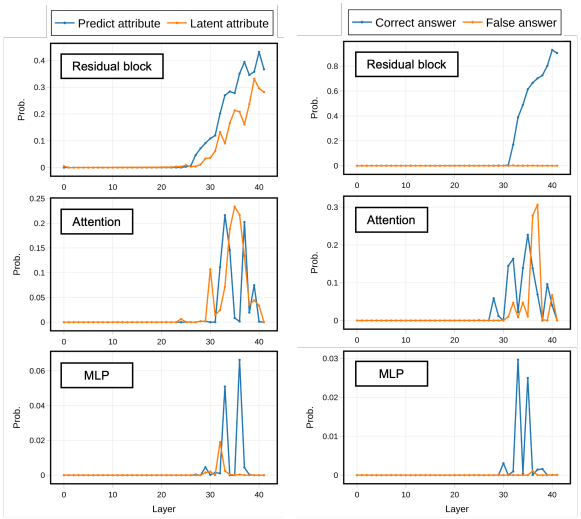

(a) (b)

Figure 10: Logit attribution results on CommonsenseQA of Gemma2-9B. (a) Probability of $\mathcal{O}_p$ and $\mathcal{O}_c$ at the position of predicting $\mathcal{O}$. (b) Probability of $\mathcal{A}_l$ and $\mathcal{A}_f$ at the position of predicting $\mathcal{A}$.

ID	Feature Explanation
115620	Phrases related to confrontation and dynamics involving identity.
99851	References to characters and elements from the Harry Potter series.
82918	Concepts related to creation and storytelling in various media.
114490	Elements related to character dynamics and development in storytelling.

Table 8: Top-scoring features decoded by SAE in the output of MLP at layer 37 when predicting $\mathcal{O}$.

Layer	ID	Feature Explanation
7	106518	References to specific characters and items from a fictional universe.
7	113897	References to characters and locations from the Harry Potter series.
32	5548	References to specific characters and events from the Harry Potter series.
32	94534	References to the concept of "world" or "global" themes

Table 9: Top-scoring features decoded by SAE in the output of MLP at layer 7 and 37 at $\mathcal{S}$.

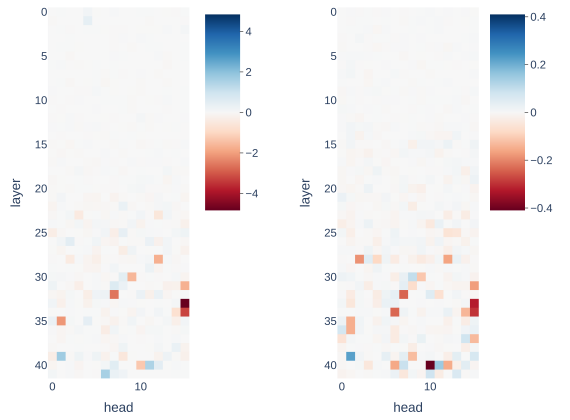

(a) Trace back at $\mathcal{A}$ (to $\mathcal{O}$) (b) Trace back at $\mathcal{O}$ (to choices)

Figure 11: Distribution of key heads (Gemma2-9B) during tracing back at different token positions on SocialIQA (averaged on 100 samples). The red squares indicate heads that have a significant positive impact on predicting the output token.

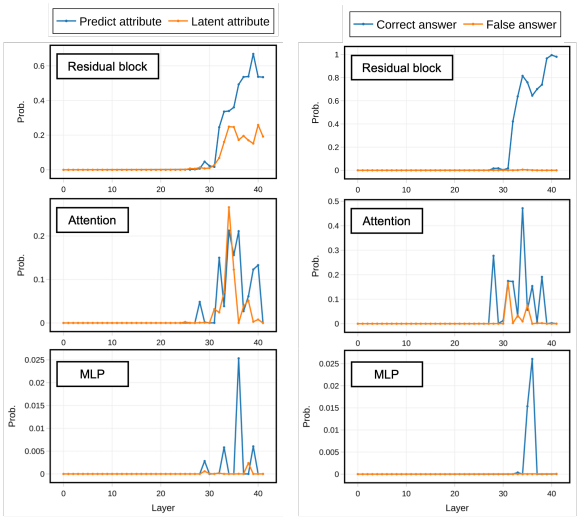

(a) (b)

Figure 12: Logit attribution results on SocialIQA of Gemma2-9B. (a) Probability of $\mathcal{O}_p$ and $\mathcal{O}_c$ at the position of predicting $\mathcal{O}$. (b) Probability of $\mathcal{A}_l$ and $\mathcal{A}_f$ at the position of predicting $\mathcal{A}$.

Head	Top tokens in projection
25.01	`Hogwarts, wizard, wizards, children,`
25.02	`Brito, British, London, Westminster`
29.06	`book, chapters, books, Book, bookId`
29.14	`wizards, wizard, Hogwarts, Harry`

Table 10: Top-scoring tokens in the key attention heads output when predicting $\mathcal{O}$. (i.e., "*fictional character*" for "*Harry Potter*".)

Table 11: SSFT results using CommonsenseQA as the training dataset.

Models	Tuned Params.	ID Task		OOD Task							
		CSQA		Winogrande		StrategyQA		SocialIQA		Average	
		Acc.	Δ	Acc.	Δ	Acc.	Δ	Acc.	Δ	Acc.	Δ
Gemma2-9B	-	75.7	-	61.2	-	70.7	-	73.0	-	68.3	-
+ SFT	9B	81.3	+5.6	59.8	-1.4	71.0	+0.3	77.4	-5.6	66.1	-2.2
+ SSFT	0.2B	82.1	+6.4	65.1	+3.9	70.7	-	74.3	+1.3	70.0	+1.7
Llama2-7B	-	61.1	-	62.5	-	53.4	-	60.2	-	58.7	-
+ SFT	6.7B	72.3	+11.2	57.8	-4.7	53.5	+0.1	55.7	-3.0	56.2	-2.5
+ SSFT	0.2B	73.5	+12.4	63.1	+0.6	56.2	+2.8	63.2	+3.0	61.8	+3.1

Table 12: SSFT results using SocialIQA as the training dataset.

Models	Tuned Params.	ID Task		OOD Task							
		SocialIQA		Winogrande		StrategyQA		CSQA		Average	
		Acc.	Δ	Acc.	Δ	Acc.	Δ	Acc.	Δ	Acc.	Δ
Gemma2-9B	-	73.0	-	61.2	-	70.7	-	75.7	-	69.2	-
+ SFT	9B	80.2	+7.2	59.0	-2.2	72.0	+1.3	72.1	-3.6	67.7	-1.5
+ SSFT	0.2B	81.1	+8.1	64.2	+3.0	70.9	+0.2	77.0	+1.3	70.7	+1.5
Llama2-7B	-	61.1	-	62.5	-	53.4	-	60.2	-	58.7	-
+ SFT	6.7B	72.3	+11.2	57.8	-4.7	53.5	+0.1	55.7	-3.0	56.2	-2.5
+ SSFT	0.2B	73.5	+12.4	63.1	+0.6	56.2	+2.8	63.2	+3.0	61.8	+3.1

Table 13: Examples of Reasoning Cases from CommonsenseQA and SocialIQA Datasets. The answer is generated by Gemma2-9B. In CommonsenseQA and SocialIQA, the entities are often abstract names or professions with no specific meaning. Therefore, we treat the options in the context as attributes, the final predicted option as the predicted attribute, and the remaining options as candidate objects.

Dataset	CommonsenseQA	SocialIQA
Question	The artist was sitting quietly pondering, then suddenly he began to paint when what struck him? (A) sadness (B) anxiety (C) inspiration (D) discomfort (E) insights	remy had a good talk with aubrey so aubrey understood remy better now. How would Remy feel as a result? (1) unsatisfied (2) calm (3) anxious
Answer	The **artist** was sitting quietly pondering, then suddenly he began to paint when **inspiration** struck him. So the answer is: (C) inspiration.	**Remy** had a good talk with Aubrey. Thus, Aubrey understands Remy better. Remy will feel **calm** as a result. So the answer is: (2) calm.
Answer Type	Multiple Choice	Multiple Choice
Answer Token	(C) inspiration	(2) clam
Concept	artist	Remy
Predicted Object	inspiration	calm
Candidate Object	sadness, anxiety, discomfort	unsatisfied, anxious

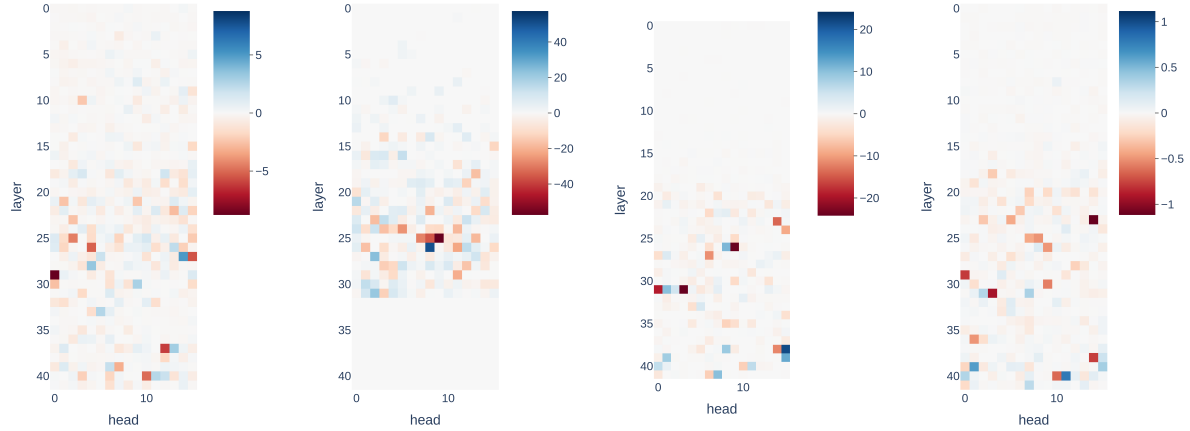

(a) Trace back at $\mathcal{O}$ (to $\mathcal{S}$) (b) Trace back at $\mathcal{R}$ (to $\mathcal{O}$) (c) Trace back at $\mathcal{C}$ (to $\mathcal{R}$) (d) Trace back at $\mathcal{A}$ (to $\mathcal{C}$)

Figure 13: Distribution of key heads during tracing back at different token positions on StrategyQA (averaged on 100 samples). The red squares indicate heads that have a significant positive impact on predicting the output token.

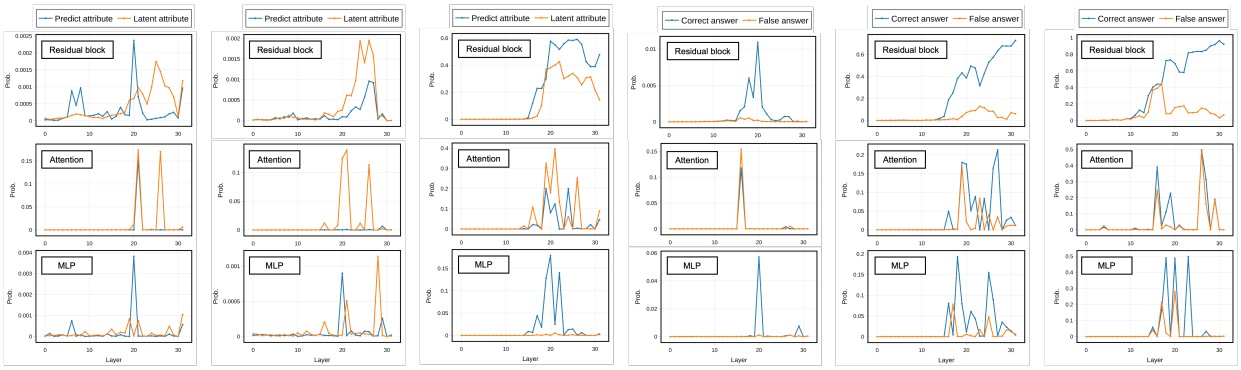

(a) (b) (c) (d) (e) (f)

Figure 14: Logit attribution results on StrategyQA of Llama2-7B. (a) Probability of $\mathcal{O}_p$ and $\mathcal{O}_c$ at $\mathcal{C}$. (b) Probability of $\mathcal{O}_p$ and $\mathcal{O}_c$ at the end of question. (c) Probability of $\mathcal{O}_p$ and $\mathcal{O}_c$ at $\mathcal{O}$ prediction. (d) Probability of $\mathcal{A}_l$ and $\mathcal{A}_f$ at $\mathcal{R}$. (e) Probability of $\mathcal{A}_l$ and $\mathcal{A}_f$ at $\mathcal{S}$ prediction. (d) Probability of $\mathcal{A}_l$ and $\mathcal{A}_f$ at $\mathcal{A}$ prediction.

Table 14: Examples of Reasoning Cases from StrategyQA Datasets. The answer is generated by Gemma2-9B.

Dataset	**StrategyQA**
Question	Is **Ganesha** associated with a Norse god?
Answer	Ganesha is a **Hindu** god. Norse gods are associated with Norse mythology. Thus, Ganesha is not associated with a Norse god. So the answer is no.
Answer Type	Yes / No
Answer Token	no
Concept	Ganesha
Predicted Object	Hindu
Candidate Object	elephant, deity, god

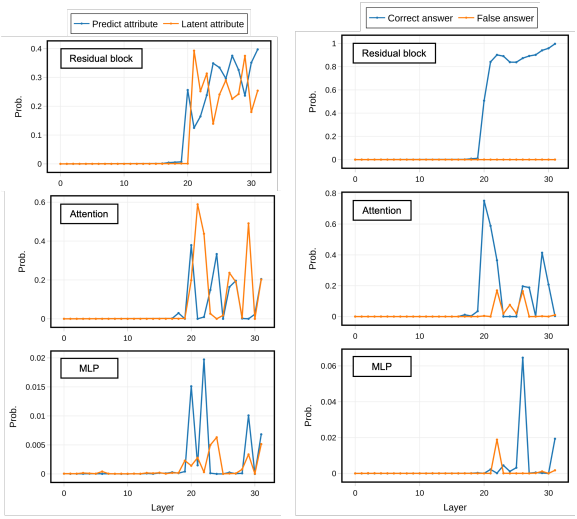

(a) (b)

Figure 15: Logit attribution results on SocialIQA of Llama2-7B. (a) Probability of $\mathcal{O}_p$ and $\mathcal{O}_c$ at the position of predicting $\mathcal{O}$. (b) Probability of $\mathcal{A}_l$ and $\mathcal{A}_f$ at the position of predicting $\mathcal{A}$.

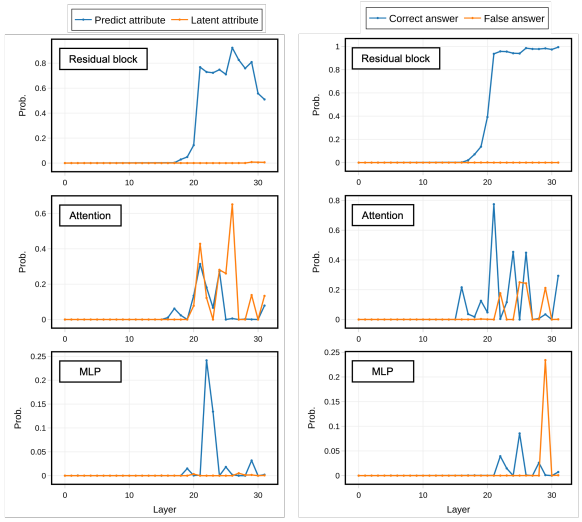

(a) (b)

Figure 17: Logit attribution results on CommonsenseQA of Llama2-7B. (a) Probability of $\mathcal{O}_p$ and $\mathcal{O}_c$ at the position of predicting $\mathcal{O}$. (b) Probability of $\mathcal{A}_l$ and $\mathcal{A}_f$ at the position of predicting $\mathcal{A}$.

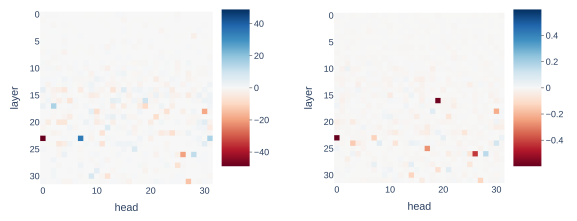

(a) Trace back at $\mathcal{O}$ (b) Trace back at $\mathcal{A}$ (to $\mathcal{O}$)

Figure 16: Distribution of key heads (Llama2-7B) during tracing back at different token positions on SocialIQA (averaged on 100 samples). The red squares indicate heads that have a significant positive impact on predicting the output token.

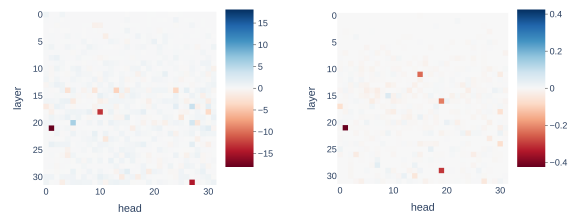

(a) Trace back at $\mathcal{O}$ (b) Trace back at $\mathcal{A}$ (to $\mathcal{O}$)

Figure 18: Distribution of key heads (Llama2-7B) during tracing back at different token positions on CommonsenseQA (averaged on 100 samples). The red squares indicate heads that have a significant positive impact on predicting the output token.

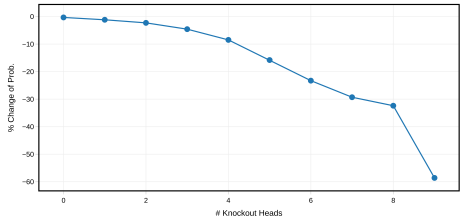

(a) Knockout top 10 heads when predicting $\mathcal{A}$

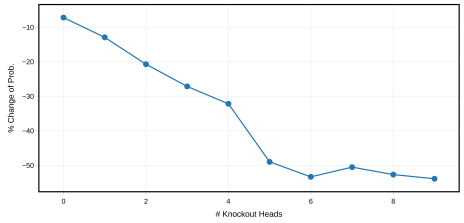

(b) Knockout top 10 heads when predicting $\mathcal{O}$

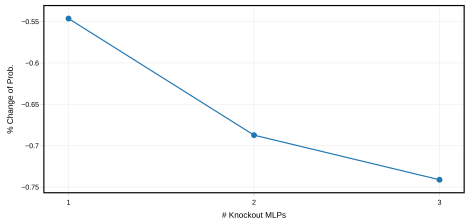

(c) Knockout top 3 MLPs when predicting $\mathcal{O}$

Figure 19: Knockout results on Gemma2-9B: (a) Decrease in probability of $\mathcal{A}_t$ when cumulatively intervene the top 10 heads for generating $\mathcal{A}$. (b) Decrease in probability of $\mathcal{O}_p$ when cumulatively intervene the top 10 heads for generating $\mathcal{O}$. (b) Decrease in probability of $\mathcal{O}_p$ when cumulatively intervene the top 3 MLPs for generating $\mathcal{O}$.

Input	Question: John cannot run the entire length of the track, he had been used to the field. The _ is short. (1) track (2) field Answer: A person who cannot run the entire length of a track likely feels uncomfortable or out of practice on a surface that is different from what they are used to. If John had been used to the field, it suggests that he is more accustomed to that environment. Therefore, the track must be
SSFT model output	**longer** than the field, making it difficult for him to run its entire length. ✅
Base model output	**shorter** than the field, as he struggles to run its entire length. ❌

(a) Case study: output of SSFT and Base model

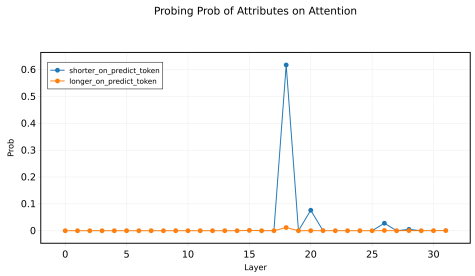

(b) Probing attention layer output for "shorter" and "longer" on SSFT model

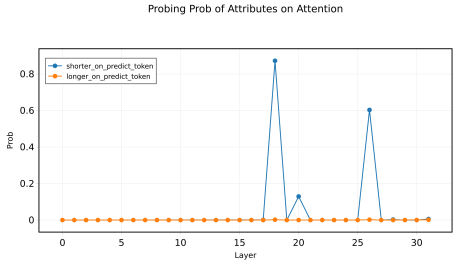

(c) Probing attention layer output for "shorter" and "longer" on Base model

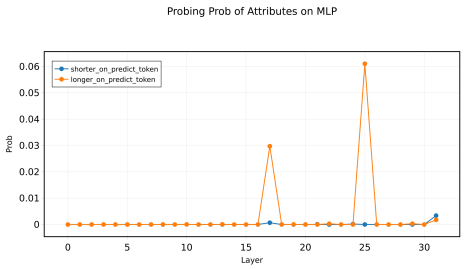

(d) Probing MLP layer output for "shorter" and "longer" on SSFT model

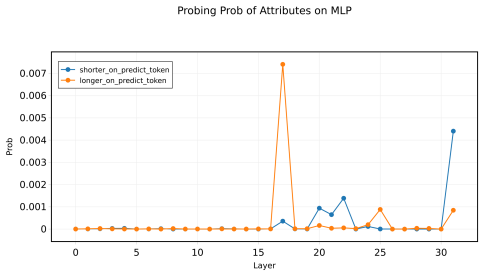

(e) Probing MLP layer output for "shorter" and "longer" on Base model

Figure 20: Comparison between the SSFT and Base models: (a) Case study highlights that the SSFT model correctly predicts the answer, while the Base model fails. (b, c) Probing results for attention layers show enhanced knowledge retrieval in the SSFT model compared to the Base model. (d, e) Probing results for MLP layers demonstrate improved reranking capability in the SSFT model. These findings confirm that the identified modules—attention heads for knowledge retrieval and MLP layers for reranking—are critical for accurate reasoning and were effectively strengthened through SSFT.

Prompt Template for Failure Case Classification

````
I am testing the accuracy of a large language model's responses on the multi-hop reasoning dataset, StrategyQA. Your task is to
classify the errors in the model's answers based on specific error types. For each question, I will provide the input question,
the model's answer, the correct answer and the reasoning steps needed for the correct answer. Your goal is to accurately classify
the errors using the following four error types:

1. **Entity Selection Error**: This occurs when the model picks the wrong entity from the input, leading to incorrect reasoning
in subsequent steps.
# Example 1:
Input:
```json
{
    "question": "Are the majority of Reddit users familiar with the Pledge of Allegiance?",
    "model_answer": "The Pledge of Allegiance is a pledge to the United States. Reddit is a social media site. Thus,
    the majority of Reddit users are not familiar with the Pledge of Allegiance. So the answer is no.",
    "correct_answer": "yes",
    "decomposition": [
        "What country do most Reddit users come from?",
        "What country is the Pledge of Allegiance associated with?",
        "Is #1 the same as #2?"
    ]
}
```
Classification: {"type": "Entity Selection Error", "explanation": "The model incorrectly selected Reddit as the entity
it spoke about, while the correct entity for reasoning should be 'Reddit users.' Therefore, this question should
be classified as an 'Entity Selection Error'".}

2. **Knowledge Retrieval Error**: This occurs when the model retrieves irrelevant, incomplete, or incorrect knowledge,
leading to flawed conclusions in the reasoning process.
# Example 1:
...

# Example 2:
...

3. **Conclusion Misalignment Error**: This occurs when the model's reasoning steps are correct, but the final conclusion is wrong.
# Example 1:
...

4. **Reasoning Logic Error**: This occurs when the logical connection between the reasoning steps and the final
conclusion breaks down. In this error, even if individual reasoning steps are correct, they fail to coherently lead
to the intended conclusion, causing the reasoning process to result in an illogical or incorrect outcome.
# Example 1:
...

Instructions: If the error does not fit into any of these four categories, please suggest a new category with a clear explanation.

For each input, I will provide the question, the model's answer, the correct answer, and the decomposition of reasoning steps.
You should return your classification and a brief explanation as
follows:
```json
{"type": "Entity Selection Error" or "Knowledge Retrieval Error" or "Conclusion Misalignment Error" or
"Incomplete Reasoning Error", "explanation": "Explain why this question belongs to the chosen category."}
```
Classficiation:
````

Figure 21: Prompt for using GPT-4 to automatically classify the category of failure case.